Biochemical and Biophysical Research Communications 423 (2012) 857–862

Contents lists available at SciVerse ScienceDirect

Biochemical and Biophysical Research Communications

journal homepage: www.elsevier.com/locate/ybbrc

Steric–electronic effects in malarial peptides inducing sterile immunity

Armando Moreno-Vranich [a], Manuel E. Patarroyo [a,b,*]

[a] Fundación Instituto de Inmunología de Colombia (FIDIC), Bogotá, Colombia
[b] Universidad Nacional de Colombia, Bogotá, Colombia

ARTICLE INFO

Article history:
Received 8 June 2012
Available online 17 June 2012

Keywords:
Clashes
Steric-hindrance
Ramachandran-plots
Critical-residues
Molecular geometry

ABSTRACT

Conserved *Plasmodium falciparum* high activity binding peptides' (HABPs) most relevant proteins involved in malaria parasite invasion are immunologically silent; critical binding residues must therefore be specifically replaced to render them highly immunogenic and protection-inducing. Such changes have a tremendous impact on these peptides' steric–electronic effects, such as modifications to peptide length peptide bonds and electronic orbitals' disposition, to allow a better fit into immune system MHCII molecules and better interaction with the TCR which might account for the final immunological outcome.

1. Introduction

Malaria (mainly that caused by the *Plasmodium falciparum* parasite) continues being one of the main public health problems around the world, causing about 200 million cases and 1.2 million deaths per year [1]. A totally effective vaccine against this devastating disease is thus desperately needed.

A series of rules and principles had thus been developed by our institute during the last 30 years for obtaining a multi-epitope, multi-stage, minimal subunit-based, chemically-synthesised, fully-protective, antimalarial vaccine [2]. The first rule involved analysing (at atom level) chemically-synthesised, short amino acid sequences (~20 mer long) derived from the most relevant proteins involved in this parasite's invasion of red blood cells (RBC) [3] and hepatocytes [4] presenting high binding ability, so-called high activity binding peptides (HABPs). The second rule determined that, due to the parasite's tremendous genetic variability in certain of these proteins' regions, conserved HABPs had to be identified and selected as components of a minimal-subunit-based, multiepitope vaccine. A third rule stated that such selection had to be corroborated by serological methods to confirm that they were immunologically silent, a fourth that their critical amino acids in host cell binding (determined by glycine analogue scanning) had to be identified and a fifth that some of these critical binding residues had to be replaced by others having similar mass and volume but opposite polarity to ensure that they would become highly immunogenic and protection-inducing [2].

The sixth rule stated that such critical amino acids must include fundamental residues [5] forming H-bonds with conserved HABPs from the same protein to create the niche where a cell's receptor fits or form part of other molecules' enzymatic site or be components of *P. falciparum* export element (PEXEL) motifs etc. In essence, they had to form part of molecules' regions which would be biologically-relevant in invasion to become disrupted by an immune response.

Such specific replacement of critical amino acids would ensure that modified, highly-immunogenic, protection-inducing HABPs were obtained when immunising *Aotus* monkeys preceding experimental challenge, thereby making them fundamental components in obtaining a fully protective vaccine against malaria.

A seventh rule stated that such changes would dramatically modify these HABPs' ability to bind to major histocompatibility complex class II (MHCII) antigen-presenting molecules, also known as HLA-DRβ1 in humans [6], to constitute a highly stable trimolecular complex with the T-lymphocyte receptor (TCR) (i.e. the MHCII–peptide–TCR complex [7]) which can appropriately activate the immune system, thereby developing a protection-inducing immune response, as has been thoroughly demonstrated [2,4]. These MCHII molecules have a peptide binding region (PBR) into which a 9 amino-acid-long peptide segment must fit to properly accommodate the downwardly-orientated corresponding amino acids (herein coloured according to their localisation in Fig. 2) into so-called pocket 1 (fuchsia), pocket 4 (dark blue), pocket 6 (orange) and pocket 9 (green). The upwardly-orientated or solvent-exposed residues, named P2 (red), P3 (pale blue), P5 (pink), P7 (yellow), are putative TCR-contact residues.

Comparative 3D structure studies at our institute using ^{1}H NMR, covering 150 of the aforementioned modified and native HABPs

* Corresponding author at: Fundación Instituto de Inmunología de Colombia (FIDIC), Bogotá, Colombia. Fax: +57 1 4 81 52 69.
E-mail address: mepatarr@mail.com (M.E. Patarroyo).

0006-291X/$ - see front matter © 2012 Elsevier Inc. All rights reserved.
http://dx.doi.org/10.1016/j.bbrc.2012.06.054

have revealed dramatic changes in their 3D structure, such as α-helix displacement and/or shortening, β-turn formation in random-structured conserved HABPs, modifications of β-turns, etc. [2].

Due to the tremendous complexity of MHCII–peptide–TCR interactions at electronic and structural level it was decided to make a comparative study on the steric–electronic effects caused by such modifications on highly relevant merozoite surface protein 1 (MSP-1) conserved HABP (1585) which is deeply involved in the parasite's invasion of RBC [2,3,8].

Therefore non-immunogenic, non-protection-inducing conserved HABP 1585 [8] (sequence EVLYLKPLAGVYRSLKKQLE, with critical binding residues underlined) and one of its modified analogues, highly-immunogenic **10014** (sequence EVLYHVPLAGVYRSLKKQLE) proving to be protection-inducing against experimental challenge in *Aotus* monkeys, were selected for the present studies; their 3D structure had already been determined by ^{1}H NMR [8].

2. Materials and methods

Peptide synthesis has been thoroughly described and in-depth immunological studies carried out [2,5], as has ^{1}H NMR-determined 3D structure of HABP 1585 and **10014** [8]. A comparative study of Φ and ψ angles for selected conformers be seen in the Supplementary Table are available on request.

A group of conformers obtained by ^{1}H NMR restrictions was analysed using Insight II (ACCELLRysInc, Software, USA); the one having the lowest energy was chosen and its data was exported in Word format.wrl to be rendered in 3D studio MAX Auto desk (Auto desk Inc).

3. Results and discussion

3.1. Immunological studies

Specifically-modified conserved HABPs being rendered highly immunogenic peptides has been thoroughly depicted: this was determined by the induction of high antibody titres (1:640 in trial 1 and 1:640 in trial 2) assessed by IFA in 1 out of 4 monkeys in trial 1 and 1 out of 5 in trial 2 when immunised with modified HABP **10014** [8].

These antibodies have recognised membrane structures in *P. falciparum* schizont-infected RBC (determined by IFA) corresponding to the cellular localisation of MSP-1 from which conserved HABP 1585 amino acid sequence was derived (Fig. 1A).

Such antibodies have reacted in Western blot analysis of *P. falciparum* merozoite lysate molecules having molecular weights corresponding to the MSP-1 protein (195 kDa) or its 70 and 42 kDa cleavage fragments where 1585 amino acid sequence is located (Fig. 1B).

More importantly, monkeys developing these high antibody titres in both trials were the very ones which became fully-protected against challenge with 100,000 freshly-obtained infected erythrocytes from a highly virulent *Aotus*-adapted *P. falciparum* strain. However, no antibodies as determined by Western blot (Fig. 1C) or IFA (data not shown) or protection have been induced when *Aotus* monkeys were immunised with native HABP 1585 [8].

This data confirms once again that native conserved HABPs like 1585 are not immunogenic, nor protection-inducers, and that their critical binding residues must be specifically modified (i.e. **10014**) to render them highly immunogenic and protection-inducing.

3.2. Native and modified HABP 3D structure

^{1}H NMR studies of 1585 [8] revealed an α-helical region from residues Tyr4 to Tyr12 displaying two α-helixes (Fig. 2A) containing critical binding residues Leu5, Lys6, Pro7 and Ala9 while **10014** had a polyproline II-like structure in the same region [9] (Fig. 2B).

Although side-chain conformation reliability (as assessed by ^{1}H NMR) was limited by relatively high conformational freedom, the interatomic distance between the most distant Tyr4 and Tyr12 atoms in the 1585 conformer (Fig 2A) was 16 Å, too short to properly fit into pockets 1–9 of these MHCII molecules which have a 25.0 ± 3.5 Å distance. Such data has been corroborated by the inability of 1585 to experimentally bind to any of the class II purified molecules studied so far [2,8]. Conversely, **10014** (His5Leu and Val6Lys replacements) had a more flexible structure in the critical binding residue region, displacing the α-helical region 6 residues backwards from Ala9 to Gln18 [8]. The polyproline II-like structures' distance between Tyr4 and Tyr12 was 26.6 Å in **10014**, a perfect distance to fit into any class II molecule pocket 1–9, as elegantly shown by others [6,7,9].

Striking differences in side-chain orientation have also been observed between these two peptides (Fig. 2A and B). When taking Tyr4 as the first residue, based on highly immunogenic **10014** binding motifs and registers, Leu5 (red) was orientated horizontally and towards the left-hand side in 1585, while replaced His5 in **10014** (theoretically the P2 TCR contacting residue, in red) was orientated upwards and towards the right-hand side (Fig. 2B and E). Similarly, while Lys6 in 1585 was almost perpendicularly orientated towards the peptide backbone (Fig. 2A and C), replaced Val6 in **10014** (the putative P3 TCR contacting amino acid) was orientated horizontally, slightly upwards and towards the left-hand side (Fig. 2B and E).

Some distant effects regarding such replacements were also observed for these two peptides outside the replaced residues' region; for example, Leu8 (pink) was downwardly orientated in 1585 while central and upwardly orientated in **10014** and Val11 (yellow) was orientated downwards and towards the right-hand side in 1585, whilst being upwardly orientated and towards the left-hand side in **10014.** Both amino acids were putative P5 and P8 TCR contacting residues, respectively, suggesting that such modifications had mainly been made in TCR contacting residues, and that modifications might have a long-term structural and biological effect.

All structural differences (peptide length and residue orientation) may partially explain both peptides' differing immunological behaviour to ensure a proper fit into the MHCII–peptide–TCR complex [7].

3.3. Analysing subatomic electronic and steric effects

Steric–electronic effect analysis of both peptides revealed (Fig. 2C) three C_6 bonds (yellow) in Tyr4 (common to 1585 and **10014,** theoretically fitting into Pocket 1 according to MHC II molecule binding motifs and binding registers) in the front view of 1585; these had *sp2* hybridisation (amplified in Fig. 2D) interacting with C_1 and C_5, each generating a 120° torsion angle.

C_6 initial electron configuration situated a pair of valence electrons in *2s* atomic orbital, 1 electron in *2px* orbital and another in *2py* orbital, promoting a *2s* orbital electron to *2pz* orbital to form 3 *sp2* hybrid orbitals having the same energy level to interact in equilibrium with their 3 neighbouring atoms, one electron thus remaining in *2pz* orbital. These hybrid orbitals interacted with hybrid orbitals from immediately neighbouring C-atoms to form sigma bonds σ (shown in yellow throughout this manuscript), in this case connecting C_6–C_1 and vice versa along these two carbons' internuclear axis. Something similar occurred between C_6 and C_5,

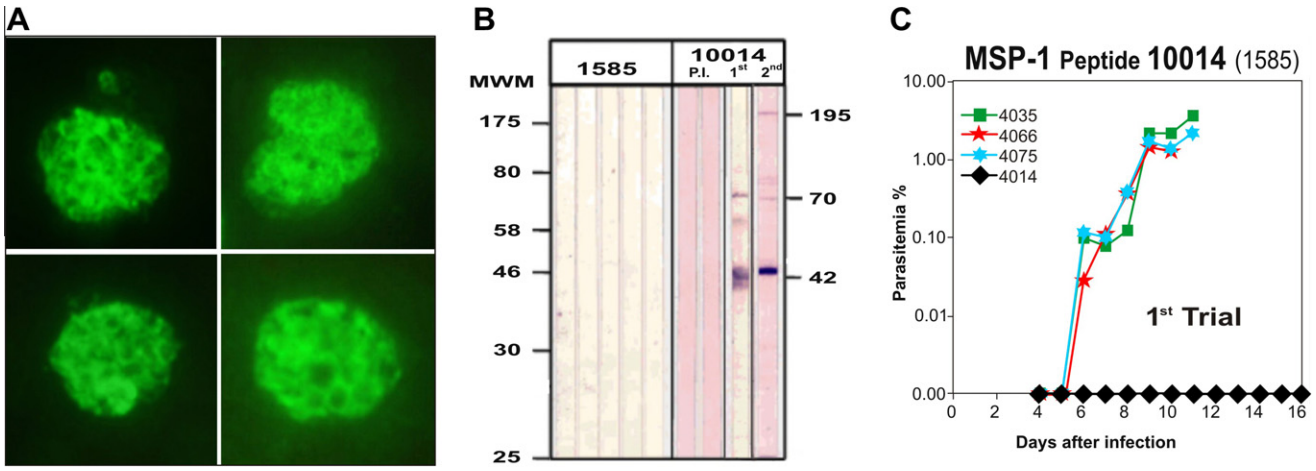

Fig. 1. (A) MSP-1 immunofluorescence pattern and membrane localisation in *P. falciparum* schizont-infected RBCs detected with *Aotus* sera immunised with **10014**. (B) Western blot analysis of *P. falciparum* merozoite protein lysate with sera from *Aotus* monkeys immunised with either 1585 or modified HABP **10014.** (C) The course of parasitaemia on a semi-logarithmic scale in *Aotus* monkeys immunised with fully-protective **10014** in trial 1, where one monkey out of four (*Aotus* 4014), having very high IFA antibody titres and strong reactivity by Western blot, was fully protected. Similarly, one of the five **10014-**immunised *Aotus* monkeys was fully protected in trial 2 (data not shown).

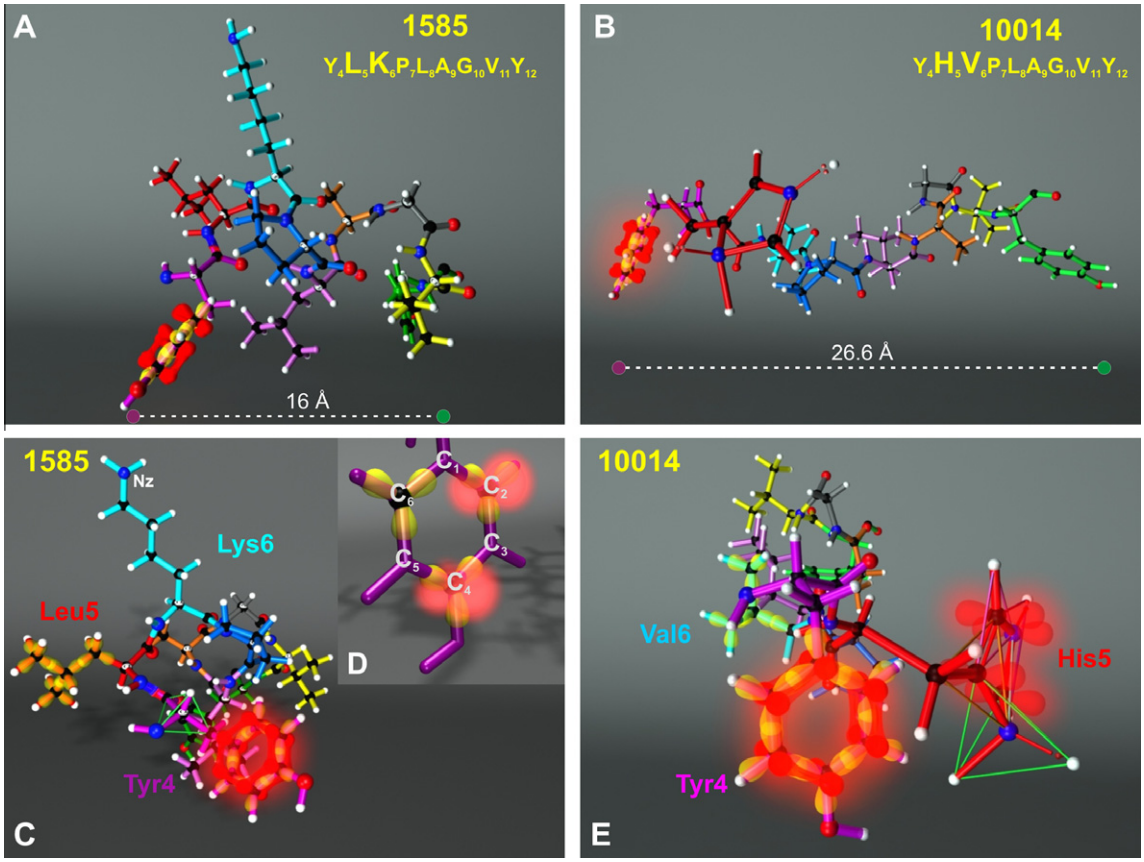

Fig. 2. 3D structure of 1585 and **10014** peptide's lowest energy conformers, theoretically fitting into MHCII–peptide–TCR complex as assessed by ^{1}H NMR. (A) and (B) side views displaying the side-chain atoms. (C) native 1585 with Tyr4 enlarged in insert, (D) displaying hybrid orbitals in yellow and *p* orbitals perpendicular to them (in red balloons). (E) The same Tyr4 in **10014** displaying π resonance in red and trigon I (yellow), II (dark blue) and III (pink) upward orientation in His5, and *p* orbital localisation. Colour code for amino acids throughout this paper: Tyr4 (fuchsia), Leu5His (red), LyS6Val (pale blue), Pro7 (dark blue), Leu8 (pink), Ala 9 (orange), Gly10 (gray), Val11 (yellow) and Tyr12 (green).

such pattern being common throughout the whole extension of the Tyr4 ring and also between some C-atoms, such as C_3, C_5 and C_6, interacting with *s* orbitals from their neighbouring hydrogens (H). However, the electron remaining in the C_6 *pz* orbital played an important role in the Tyr4 rings' resonance structure as the charge became balanced to form the π bonds resulting from overlapping bonds between 2*p* orbitals located perpendicularly to the internuclear axis. Consequently, as each *p* orbital alternated in such overlapping, then the electron charge was uniformly distributed, thereby inducing resonance (Fig. 2C and E).

O_7 geometry was tetrahedral in Tyr4 in spite of visually seeming to have bend geometry as this O_7 was bound to C_4 and to an H; however, considering its 2 non-bonding electron pairs, these were orientated in H towards a bend position, instead of being projected in a straight position with O_7. A Cβ centred in a tetrahedron, in whose vertices Cα and 2H were located, was found on the opposite side of the ring.

The following 1585 residue was Leu5 in which all its C interacted by means of single σ-bonds (Fig. 2C) where Leu5 geometry began with the R side-chain (Fig. 3A); it can be seen that each CH3 (Cδ 1 and Cδ 2) was framed within a tetrahedron (green) in whose vertices were located 3H and one C (from CγH). The geometry for each C-atom (Cα, Cβ and Cα) of this apolar aliphatic chain behaved in the same way. Something similar occured with Cα4 where the hybridisation of each carbon involved one *2s* orbital and 3 *2p* orbitals (i.e. as C was able to bind to 4 neighbouring atoms, 4 *sp3* hybrid orbitals developed to form the same number of σ-bonds with each neighbouring atom) (Fig. 2C yellow orbitals in Leu5). The tetrahedrons orientating the two trigons on the plane 4 where the peptide bond occurred projected the plane on which each corner was occupied by Cα4, Oc=o, Cα3 and Cδ (Fig. 3B).

The geometry inherent to Lys6 (the next residue) was the same as that described for C in Leu5, the geometrical difference lying in *Nz* from this Lys, since N atomic number 5 indicated that when it had contacted three neighbouring atoms, only a non-bonding electron pair remained, playing a role in this amino acid's trigonal pyramidal geometry (data not shown).

Two trigons were observed on the plane (Fig. 3B) of the next residue, common to 1585 and **10014** peptides, when considering Pro7 geometry whose ring was horizontally projected towards the right (Figs. 2A and B and 3B) so as to theoretically fit into MHCII pocket 4; one trigon was formed by Cα3, Oc=o adjacent to Nα4 and Nα4 itself, whilst Cc=o was located in the vertex of the other trigon (pink), demarked by Cα4, Cc=o, the plane not being bound to H which is conventionally bound to N due to the resonance structure produced by electron delocalisation between Oc=o, Cc=o and Nα2 and the fact that Pro structure is cyclic instead of being aliphatic. The atom framed in the centre of the trigon, Nα4, bound to 3 neighbouring atoms to minimise electron repulsion, meaning that after promoting an electron from *s* orbital to *p* orbital, such *s* orbital became hybridised with 2 of the *p* orbitals, thereby obtaining 3 hybrid orbitals with which to interact with their neighbours, establishing 3σ-bonds, whilst the remaining electron or electrons became available in a *p* orbital perpendicularly situated to the internuclear axis connecting Nα4 to Cc=o. The same thing happened with an π orbital perpendicular to the intern clear axis between Cc=o and Oc=o; this O was also circumscribed in a trigon described by Cc=o and its 2 free electron pairs.

The presence of Pro7 conferred rigidity on this part of the molecule since Cα and Cδ contiguous to Nα4 formed a direct part of the plane; turning this plane would thus contemplate much more steric repulsion on moving the whole R group. The geometry for each of its C was tetrahedral.

Leu8 had similar geometry in all its C to that described for Leu5, this being repeated in Ala9; Val11 also had tetrahedral geometry in all its C and the geometry of Tyr12 was analogous to that described in Tyr4.

The side view of modified HABP **10014** (Leu5His and Lys6Val substitutions) in Fig. 2B shows a free electron pair in the trigon vertices also observed in Fig. 3C, purple.

Fig. 3C shows how C4 interacted with N_3 in **10014** His5 via a single bond, with C5γ by a double bond and with H via a single bond having trigonal planar geometry (c. 120° c/u). From the electron point of view, as C4 interacted with 3 neighbouring atoms, it needed 3 hybrid orbitals having the same length, as well as promoting an electron from *s* orbital to *p* orbital, hybridising a *2s* orbital with 2*p* orbitals to obtain 3 *sp2* hybrid orbitals to interact with its 3 neighbouring atoms, whilst the remaining electron located in *p* orbital participated in establishing a double bond with C_2.

By contrast, N_1 established three σ-bonds, one of which bound to C2 hybrid orbital, another to $C_5\gamma$ hybrid orbital and a third to H *s*-orbital, the remaining electron pair being non-bonding. The non-bonding electron pair was situated in the vertex of the tetrahedron formed with C2, C5γ by *sp3* hybridisation and this electron pair were able to interact with a proton, thereby increasing polarity. The details of the geometry for C_2 were similar to that described for C_4.

$C_{5\gamma}$ (like C_2) was located on a trigonal plane (yellow and cyan trigons, respectively), where one of the vertices of such plane was projected towards the centre of the tetrahedron circumscribing N_1.

His5 *p* orbital electron clouds were of vital importance in modified HABP **10014** configuration (blurred in red, Fig. 3C), where electron repulsions established four planar trigons (C_4, C_2 and $C_{5\gamma}$ and N_3) from the ring being framed in each one. N_1 was framed within a tetrahedron, but its geometry was trigonal pyramidal since Ha (represented in Fig. 3C) was really a proton which bound to an N free electron pair, so that such electrons could alternately occupy the vertex of the tetrahedron considered in such geometry. However, trigonal pyramidal geometry was attributed as free electron pairs were not taken into account here for geometric effects. All of the foregoing explained the fact that there was no resonance in His5, as the lack of *p* orbital in N_1, given interaction with its

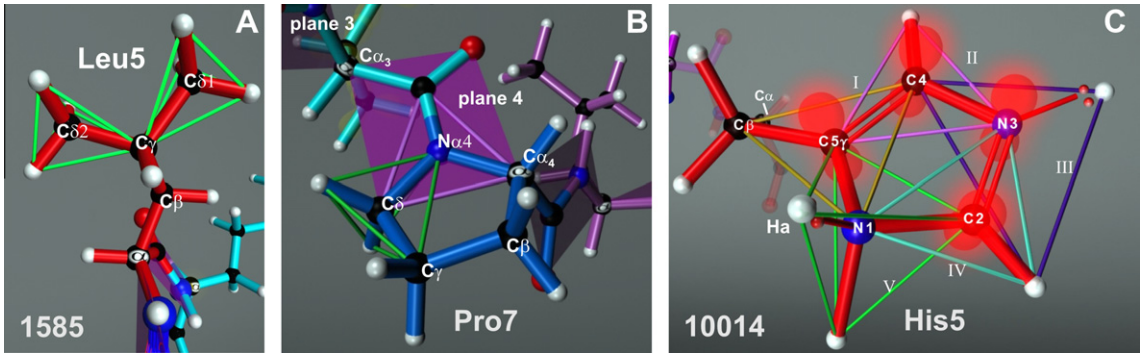

Fig. 3. (A) Tetrahedron formation in 1585 Leu5 from Cα, framing Cδ1 and Cδ2. (B) In Pro7 $C\alpha_3$ and $C\alpha_4$ orient all atoms to conform plane 4. (C) Trigon I (yellow) geometrical formation in **10014** His5 between N_1, Cβ and C_4, framing $C_5\gamma$ α; trigon II (pink) between N_3, $C_5\gamma$ and non-bonding pair, framing C_4; trigon III (dark blue) between C_4, HC_2 and the N_3 non-bonding pair framing N_3; trigon IV (pale blue) between N_1 and HC_2 and N_3 framing C_2 and tetrahedron V between C_2, $C_5\gamma$, HN_1 and non-bonding pair framing N_1. Blurred *p* orbitals perpendicular to the main atom (red).

neighbours, led to affirming that there were no electrons in some of its *px* orbitals, as happened with N_3. The latter formed a double bond with C_2 due to the effect of C_2 *px* orbital interaction with N_3 *px* orbital forming a π-bond and also the interaction of its hybrid orbitals, leaving a free electron pair in the trigon vertex (represented in purple), completing its 5 valence electrons. Consequently, as His5 had more surface-exposed or solvent-exposed *p* orbitals, the non-binding electron pair and available atoms having trigons I, II and III may thus have been those appropriately interacting with the TCR.

10014 Val6 geometry (Fig. 2B and E) was no different to that described for 1585 Val11; the same happened for the following residues from Pro7 to Tyr12 (whose geometry has already been described for peptide 1585). However, in spite of geometry being tetrahedral in Val6 (as it was for Lys6), Val6 had considerably lower 140 $Å^3$ volume than 166.7 $Å^3$ for Lys (thereby providing space for two H_20 molecules having 12.5 $Å^3$) whilst having only a difference of around 11 $Å^2$ superficially.

Fig. 4 shows an analysis of the geometry inherent in peptide bonds, whose Cc=o and Nα come into contact with MHCII amino acid side-chain atoms for stabilising peptide–MHCII bonds. Cα, located in the centre of tetrahedrons, directs the atoms participating in the amide bond ($C_{c=O}$ and Nα) placing their atoms on the same plane (i.e. Nα1 is located in the vertex of a tetrahedron circumscribing Cα1 and thus H binds to the said Nα1 deflected a few degrees from the plane). The H next to it forms part of one of the corners of the plane, this being important when considering minimisation of electron repulsions or clashes between electron clouds. Cα2 is located in the following corner of this plane.

One of the two remaining corners of the plane is occupied by Oc=o and the other by Cα1.

Trigonal planar geometry can be noted in each plane, where Oc=o, Nα1 and Cα1 can be found in one of the vertices of the two trigons, whilst the other trigon, consists of Cc=o, H from Nα2 and Cα2. The repulsions of atoms found on the plane must then be considered as they may affect the position of one or more of these atoms when energy is minimised, thus the importance of the plane's diagonal twist governed by the phi- (Φ) or psi-bond (ψ) represented in Fig. 4.

Fig. 4D shows the minimum energy position assumed by planes 1 and 2 containing Tyr4-His5 and His5-Val6 peptide bonds in the table of values, determined by ^{1}H NMR for this conformer (Supplementary material), the ψ angle was −30.3° as, when its value was 0°, it was in an angular position close to that shown in Fig. 4C, but Φ angular values also came into play, these being nothing more than the complement of inter-planar interactions ruled by steric clashes between the atoms making them up. The Φ angular value for Val6 in such table (105.1°), and thus the starting value represented in Fig. 4D (0°), led to determining a C_1–O_2 steric clash whose clashes became intolerant in the Φ range from ±45° for all ranges of ψ, as C_1 covered the scope of a CH3 in such consideration, but also made them become intolerant in clashes between H_1–O_2 in the ±90° range for both Φ and ψ, regardless of the clash between N_1–H_2, for any value for Φ between ±20° for ψ. It can also be noted that the least energy position (Hb) was closer to the R group from Val6 as there was a clash between O2 with the latter whose repulsion angular values ranged from 70° to 170° for Φ, and for the whole angular range for ψ [10,11].

By comparison, the minimum energy position for planes 1 and 2 made it evident that the Leu5 and Lys6 R positions were relevant regarding the magnitude of Φ angular value since the −65.4° for 1585 obeyed not only the O1–C2 clash but was also limited by the position of Leu5, contrary to that found for **10014** H5. Bearing

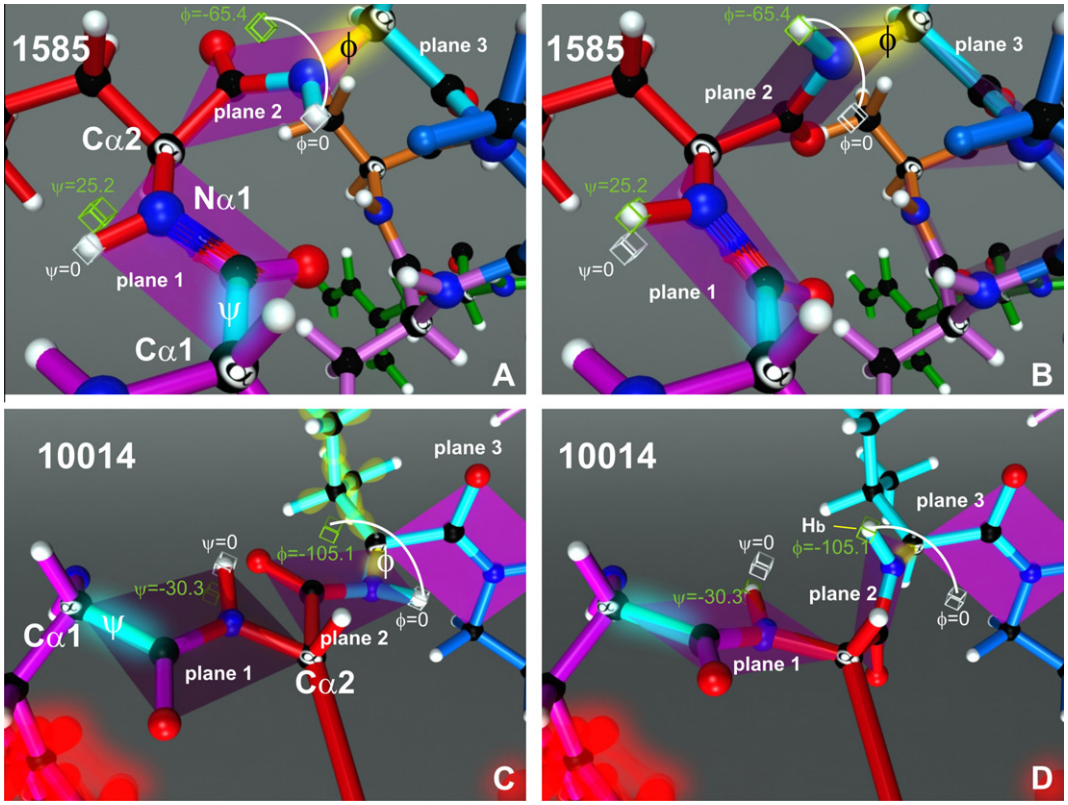

Fig. 4. Comparison of initial positions (A and C for 1585 and 10014) peptidebond atoms forming Φ and ψ angles on planes 1 and 2 represented by white cubes. (B and D for 1585 and 10014) final position represented by green cubes representing minimisation values for the atom clashes considered in the Ramachandran plots, as explained in the text.

in mind that 1585 structure is helical, steric hindrance by Pro7 regarding OC═O found in plane 2, also restricted Φ angular mobility and OC═O from plane 3 also contributed to O2–O3 clashes between ±90° ψ values and ±60° for Φ values. These types of event provide 1585 with a compact structure, ruled by steric hindrance confining its atoms in smaller spaces compared to those of **10014.**

The geometric description given here and that for electron clouds have been considered for detailing the large-scale alterations undergone by native HABPs when one critical amino acid is replaced by another, according to already established principles and rules, for a perfect fit into the MHCII–peptide–TCR complex and inducing an immune protection-inducing response, thereby leading to the development of multi-antigen, multi-stage, minimum subunit-based, chemically-synthesised vaccines, an antimalarial vaccine being one such.

Acknowledgments

We would like to thank Ms. Martha Castañeda for typing this manuscript many times and Mr. Jason Garry for translating it.

Appendix A. Supplementary data

Supplementary data associated with this article can be found, in the online version, at http://dx.doi.org/10.1016/j.bbrc.2012.06.054.

References

[1] C.J. Murray, L.C. Rosenfeld, S.S. Lim, K.G. Adrews, Global malaria mortality between 1980 and 2010: a systematic analysis, Lancet 379 (2012) (1980) 413–431.
[2] M.E. Patarroyo, A. Bermudez, M.A. Patarroyo, Structural and immunological principles leading to chemically synthesized, multiantigenic, multistage, minimal subunit-based vaccine development, Chem. Rev. 111 (2011) 3459–3507.
[3] L.E. Rodriguez, H. Curtidor, M. Urquiza, G. Cifuentes, C. Reyes, M.E. Patarroyo, Intimate molecular interactions of *P. falciparum* merozoite proteins involved in invasion of red blood cells and their implications for vaccine design, Chem. Rev. 108 (2008) 3656–3705.
[4] H. Curtidor, M. Vanegas, M.P. Alba, M.E. Patarroyo, Functional, immunological and three-dimensional analysis of chemically-synthesised sporozoite peptides as components of a fully-effective antimalarial vaccine, Curr. Med. Chem. 18 (2011) 4470–4502.
[5] M.E. Patarroyo, G. Cifuentes, C. Pirajan, A. Moreno-Vranich, M. Vanegas, Atomic evidence that modification of H-bonds established with amino acids critical for host-cell binding induces sterile immunity against malaria, Biochem. Biophys. Res. Commun. 394 (2010) 529–535.
[6] E.Y. Jones, L. Fugger, J.L. Strominger, C. Siebold, MHC class II proteins and disease: a structural perspective, Nat. Rev. Immunol. 6 (2006) 271–282.
[7] M.G. Rudolph, R.L. Stanfield, I.A. Wilson, How TCRs bind MHCs, peptides, and coreceptors, Annu. Rev. Immunol. 24 (2006) 419–466.
[8] F. Espejo, M. Cubillos, L.M. Salazar, et al., Structure, immunogenicity, and protectivity relationship for the 1585 malarial peptide and its substitution analogues, Angew. Chem. Int. Ed. Engl. 40 (2001) 4654–4657.
[9] T.S. Jardetzky, J.H. Brown, J.C. Gorga, L.J. Stern, R.G. Urban, J.L. Strominger, D.C. Wiley, Crystallographic analysis of endogenous peptides associated with HLA-DR1 suggests a common, polyproline II-like conformation for bound peptides, Proc. Natl. Acad. Sci. USA 93 (1996) 734–738.
[10] T.E. Creighton, Proteins, Structures and Molecular Properties, second ed., W.H. Freeman& Company, New York, 1996. pp. 172–176,183.
[11] S.C. Lovell, I.W. Davis, W.B. Arendall, et al., Structure validation by Cα geometry: Φ, ψ and Cβ deviation, Proteins 50 (2003) 437–450.